BNL 29840

Numerical Studies of Gauge Field Theories*

Michael Creutz
Physics Department
Brookhaven National Laboratory
Upton, Upton 11973

June 1981

*Lectures for the 19th International School of Subnuclear Physics, Erice, Italy

NUMERICAL STUDIES OF GAUGE FIELD THEORIES*

Michael Creutz+

Physics Department
Brookhaven National Laboratory
Upton, N.Y. 11973

INTRODUCTION

Monte Carlo simulation of statistical systems is a well established technique of the condensed matter physicist. In the last few years, particle theorists have rediscovered this method and are having a marvelous time applying it to quantized gauge field theories. The main result has been strong numerical evidence that the standard SU(3) non-Abelian gauge theory of the strong interaction is capable of simultaneously confinging quarks into the physical hadrons and exhibiting asymptotic freedom, the phenomenon of quark interactions being small at short distances.

In four dimensions, confinement is a non-perturbative phenomenon. Essentially all models of confinement tie widely separated quarks together with "strings" of gauge field flux. This gives rise to a linear potential at long distances

$$E(r) \underset{r\to\infty}{\sim} Kr \tag{1.1}$$

where r is the quark-antiquark separation and the constant K is

---

*The submitted manuscript has been authored under contract DE-AC02-76CH00016 with the U.S. Department of Energy.

referred to as the string tension. As K is physical, it must satisfy the renormalization group equation. This implies the form

$$K \sim \frac{1}{a^2} \exp\left(-\frac{1}{\gamma_0 g_0^2(a)}\right) (g_0^2)^{-\gamma_1/\gamma_0^2} (1 + O(g_0^2)) \qquad (1.2)$$

where g_0 is the bare coupling when an ultraviolet cutoff of length a is introduced, and the parameters γ_0 and γ_1 are the first terms in a perturbative expansion of the Gell-Mann Low function[1]

$$a \frac{\partial}{\partial a} g_0 = \gamma(g_0) = \gamma_0 g_0^3 + \gamma_1 g_0^5 + O(g_0^7) \qquad (1.3)$$

The important observation is that eq. (2) precludes any perturbative expansion of K in terms of g_0.

A non-perturbative treatment requires a non-perturbative regulator to control the ultraviolet divergences so rampant in field theory. Wilson's elegant lattice formulation provides this needed cutoff.[2] Once formulated on a lattice, the gauge theory becomes a statistical mechanics problem in which temperature corresponds to the square of the field theoretical coupling constant. It is this analogy which permits us to borrow Monte Carlo technology from the solid state physicist.

A Monte Carlo program generates a sequence of field configuration by a series of random changes of the fields. The algorithm is so constructed that ultimately the probability density for finding any given configuration is proportional to the Boltzmann weighting. We bring our lattices into "thermal equilibrium" with a heat bath at a temperature specified by the coupling constant. Thus we do computer "experiments" with four-dimensional "crystals" stored in a computer memory. As the entire field configuration is stored, we have access to any correlation function desired.

In the remainder of these lectures I will describe the kinds of experiments we have been doing and the implications of these results for strong interaction physics.

THE MODEL

We work with Wilson's formulation of a gauge field on a lattice.[2] A link variable U_{ij}, which is an element of the gauge group, is associated with every nearest neighbor pair of sites i and j on a four-dimensional hypercubic lattice. The reversed link is associated with the inverse element

$$U_{ij} = (U_{ji})^{-1} \tag{2.1}$$

The path integral

$$Z = \int \left(\prod_{\{i,j\}} dU_{ij} \right) e^{-\beta S(U)} \tag{2.2}$$

defines the quantum theory. Here we integrate over all independent link variables with the invariant group measure. The action S is a sum over all elementary squares or "plaquettes" in the lattice

$$S(U) = \sum_{\square} S \tag{2.3}$$

where for SU(N) we normalize

$$S_{\square} = \left(1 - \frac{1}{N} \mathrm{Tr}\ (U_{ij}U_{jk}U_{kl}U_{li})\right) \tag{2.4}$$

and for U(1)

$$S_{\square} = 1 - \mathrm{Re}(U_{ij}U_{jk}U_{kl}U_{li}) \tag{2.5}$$

Here i, j, k, and l label the sites circulating about the square $\square$.

In a classical continuum limit we identify

$$U_{ij} = e^{ig_o a A_\mu} \tag{2.6}$$

where a is the lattice spacing, and A_μ is the gauge potential in the direction μ which points from i to j. The potential is regarded as an element of the Lie algebra for the gauge group. In a naive continuum limit for SU(N) the action reduces to an integral over space-time of the conventional Yang-Mills Legrangian[3]

$$S = \frac{g_o^2}{2N} \int \frac{1}{4} F_{\mu\nu}^2 \ F_{\mu\nu}^2 \ d^4x \tag{2.7}$$

We refer to this limit as "naive" because for the full quantum theory the bare coupling constant must be renormalized.

Equation (2.2) is the partition function for a statistical system at temperature $T = 1/\beta = g_o^2/2N$. The most intuitive Monte Carlo algorithm consists of successively touching a heat bath at this temperature to each link of the lattice. By this I mean to take each U_{ij} in turn and replace it with a new group element U'_{ij}, selected randomly from the entire group manifold but with a weighting proportional to the Boltzmann factor

$$dP(U') \sim \exp\left[-\beta S(U')\right] dU' \tag{2.8}$$

where $S(U')$ is the action evaluated with the given link having the value U' and all other links fixed at their current values. One Monte Carlo iteration refers to the application of this procedure to each link in the entire lattice.

I have used precisely this algorithm for the SU(2) theory[4] and smaller groups. For larger groups I have found it computationally simpler to use less intuitive but standard algorithms from statistical mechanics. These are discussed in the next section and can be competitive with or better than the heat bath algorithm for groups with sufficiently complicated manifolds.

MONTE CARLO ALGORITHMS

The goal of a Monte Carlo program is to generate a sequence of field configurations in a stochastic manner so that the ultimate probability density of encountering any given configuration C is proportional to the Boltzmann weighting

$$p(c) \sim e^{-\beta S(c)} \tag{3.1}$$

where $S(c)$ is the action of the given configuration. We thus use the computer as a "heat bath" at inverse temperature β. Each state in the Monte Carlo sequence is obtained in a Markovian process from the previous configuration. Thus we have a probability distribution $P(c',c)$ of taking any configuration c into configuration c'. The

choice of $P(c',c)$ is by no means unique.[5] Most algorithms in practice change one statistical variable at a time in a manner satisfying a condition of detailed balance

$$P(c',c)e^{-\beta S(c)} = P(c,c')e^{-\beta S(c')} \tag{3.2}$$

Indeed, this condition plus an eventual access to any configuration will ultimately give the Boltzman distribution of eq. (3.1).

I will now show that an algorithm satisfying eq. (3.2) brings an ensemble of configurations closer to equilibrium. To do this, I need a definition of "distance" between ensembles. Suppose we have two ensembles E and E', each of many configurations. Suppose also that the probability density of configuration c in E or E' is $p(c)$ or $p'(c)$, respectively. Then I define the distance between E and E' as

$$||E-E'|| = \sum_c |p(c) - p'(c)| \tag{3.3}$$

where I sum over all possible configurations. Now suppose that E' is obtained from E by the Monte Carlo algorithm defined by a $P(c',c)$ satisfying eq. (3.2). This means that

$$p'(c) = \sum_{c'} P(c,c')p(c') \tag{3.4}$$

As $P(c',c)$ is a probability, it satisfies

$$P(c',c) \geq 0 \tag{3.5}$$

$$\sum_c P(c',c) = 1 \tag{3.6}$$

Note that if we sum eq. (3.2) over c' and use eq. (3.6), we obtain

$$e^{-\beta S(c)} = \sum_{c'} P(c,c')\, e^{-\beta S(c')} \tag{3.7}$$

This means that the equilibrium ensemble E_{eq}, defined by eq. (3.1), is an eigenvector of the algorithm. Using this, we can now compare the distance of E' from E_{eq} to the distance of E from equilibrium

$$\begin{aligned} ||E'-E_{eq}|| &= \sum_c \left|\sum_{c'} P(c,c')\, (p(c') - p_{eq}(c')\right| \\ &\leq \sum_{c,c'} P(c,c')\, |p(c')-p_{eq}(c')| \\ &= ||E - E_{eq}|| \end{aligned} \tag{3.8}$$

This is just the result I set out to prove; the algorithm reduces the distance of an ensemble from equilibrium.

The detailed balance condition of eq. (3.2), which is sufficient but not necessary to approach equilibrium, still does not uniquely determine P(c',c). The intuitive heat bath algorithm was discussed in the last section. In its turn, each link variable U is replaced with a new group element U' selected randomly from the gauge group with a weighting given by the Boltzmann factor

$$P(U') \sim e^{-\beta S(U')} \tag{3.9}$$

Here the action is calculated with all other links fixed, at their current values. A detailed discussion on how to implement this technique for SU(2) is given in ref. (4).

For complicated group manifolds, the heat bath generation of new elements may be too tedious to carry out efficiently, either for computational or human reasons. Several less intuitive algorithms based on the detailed balance condition have shown their value through their simplicity.[5] A popular procedure begins with the selection of a trial U' as a tentative replacement for U. This test variable is selected with a distribution $P_T(U,U')$ depending on U and symmetric in U and U'

$$P_T(U,U') = P_T(U',U) \tag{3.10}$$

Beyond this constraint, P is arbitrary and can be selected empirically to optimize convergence. Once U' is selected, the new action S(U') is calculated. If the action is lowered by the change U→U', then this change is accepted. The detailed balance condition then determines the remainder of the algorithm; if the action is raised, the change is accepted with conditional probability $\exp\{-\beta(S(U')-S(U))\}$.

To implement eq. (3.10) in practice, I usually obtain U' by multiplying U with a random group element from a table, where this table is itself of random elements with a convenient weighting towards the identity. The table contains the inverse of each of its elements. I revise this table frequently and adjust its distribution as a function of the temperature to improve convergence.

In a gauge theory, the interaction is rather complicated and involves considerable arithmetic to evaluate. Therefore it can be extremely beneficial to do as good a job as possible in selecting the stochastic changes. In terms of computer time to reach equilibrium, it is usually of value to test several trial group elements before proceeding to the next link. In this way I typically use on the order of 10 to 20 tries.

SOME "EXPERIMENTS"

I will now display the results of some simple experiments. Figure 1 shows several Monte Carlo runs with the gauge group SU(2) at the particular coupling

$$\beta = \frac{4}{g_o^2} = 2.3 \tag{4.1}$$

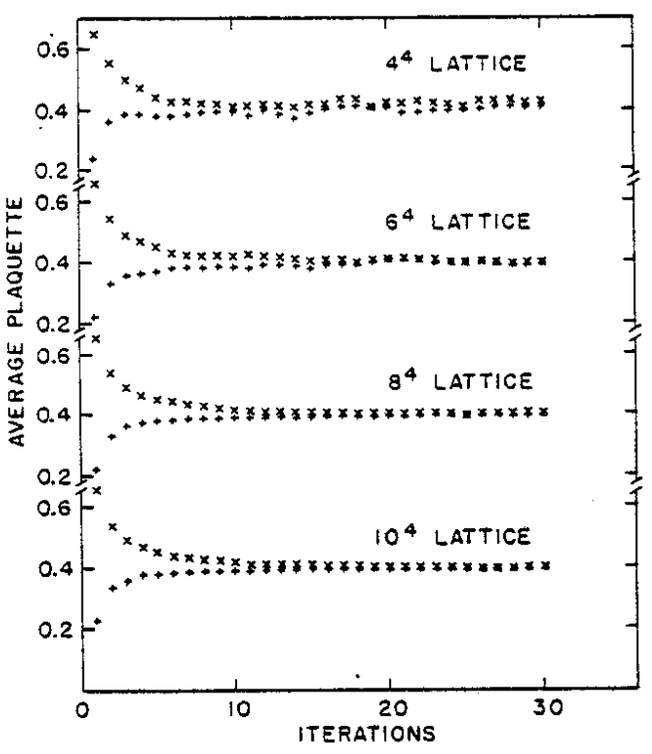

Fig. 1 The average plaquette for SU(2) gauge theory at $\beta = 2.3$ as a function of number of Monte Carlo iterations.

This value was selected as representative of the slowest convergence in this model. Runs are shown on lattices of 4^4 to 10^4 sites. I have plotted the "average plaquette" which is just the expectation value of S defined in eq. (2.4). This is shown as a function of the number of Monte Carlo iterations. For each size lattice, two different initial configurations were studied, one totally ordered with each U_{ij} set to the identity and one with each U_{ij} selected randomly from the group. Thus we approach equilibrium from opposite extremes, zero and infinite temperature. Note that for all lattice sizes convergence is essentially complete after only 20-30 iterations. Thermal fluctuations are apparent on the smallest systems but are relatively small on the 10^4 site crystal.

The situation can be much worse if a phase transition is nearby. In Fig. 2 I show the convergence of the U(1) lattice theory on a 6^4 lattice near the known critical temperature for this model. In addition to the slow convergence compared to SU(2), note the large critical fluctuations. Thus we conclude that convergence is rapid away from a phase transition and slow near one.

In Fig. 3 I show a different type of experiment. Here I have performed rapid thermal cycles on the SU(2) theory in 4 and 5 space-time dimensions and the SO(2) = U(1) theory in four dimensions.[6] Each point was obtained by running on the order of 20 iterations from an either hotter or cooler state. Phase transitions are to be suspected in regions where the heating and cooling points do not agree. Such "hysteresis" phenomena are clear for the 5 dimensional SU(2) and the four dimensional U(1) models. More detailed analysis has indicated that the U(1) transition is second order[7] and the 5 dimensional SU(2) transition is first order. Note that the 4 dimensional SU(2) model is in sharp contrast to the others. The lack of any clear hysteresis shows the critical nature of four dimensions.

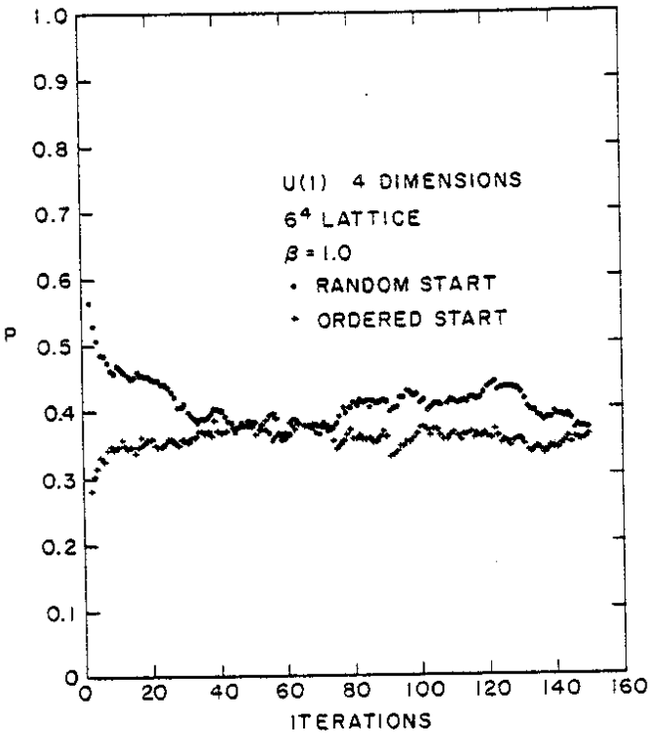

Fig. 2 The convergence of U(1) lattice gauge theory at $\beta = 1.0$.

THE STRING TENSION

As mentioned earlier, because the entire lattice is accessible, any desired correlation function can be obtained. As we are interested in the interquark potential, I can insert sources with quark quantum numbers into the lattice and measure the response. In particular, I wish to extract the coefficient K of the hypothetical long distance linear potential of eq. (1.1). Measuring distances in units of the lattice spacing, one actually measures the dimensionless combination a^2K as a function of the bare coupling. If the linear potential survives a continuum limit, the weak coupling dependence of a^2K follows from eq. (1.2). Verification of that behavior is essential to understanding confinement.

The extraction of K is made using Wilson loops. For a closed contour C of links, the Wilson loop is defined

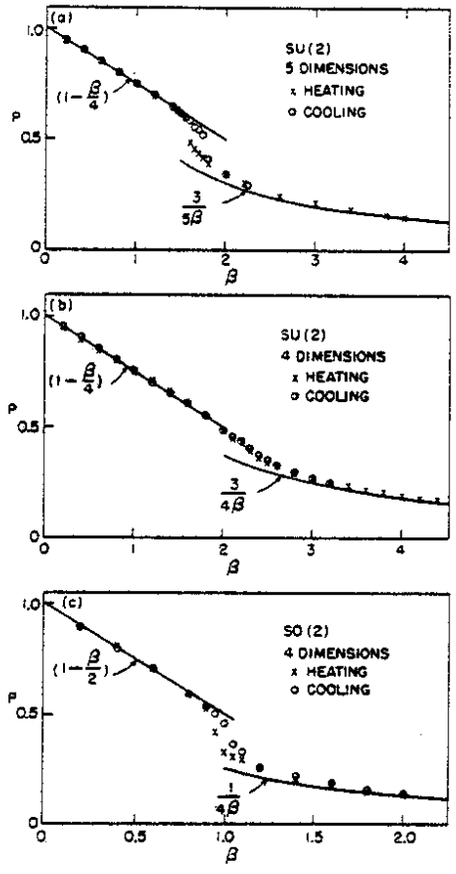

Fig. 3 Thermal cycles on several models.

$$W(C) = < \frac{1}{2} \mathrm{Tr} \ (\prod_{C} U)_{P.O.} > \tag{5.1}$$

Here P.O. represents "path ordering"; that is, the U_{ij} are ordered and oriented as they are encountered in circulating around the contour. If, for large separations, the interaction energy of two static sources in the fundamental representation of the gauge group increases linearly with distance, then, for large contours, one expects

$$\ell n \ W(C) = -K \ A(C) + 0 \ (p(C)) \tag{5.2}$$

where A(C) is the minimal area enclosed by C and p(C) is the perimeter of C. The constant K is precisely the desired string tension.

Thus motivated, I measured the expectation values of rectangular loops W(I,J) when I and J are the dimensions of the loop in lattice units.[8] From these loops I construct the quantities

$$\chi(I,J) = \ln\left(\frac{W(I,J)W(I-1,J-1)}{W(I,J-1)W(I-1,J)}\right). \tag{5.3}$$

In this combination overall constant factors and perimeter behavior cancel out. Whenever the loops are dominated by an area law, X(I,J) directly measures the string tension

$$\chi \to a^2K \tag{5.4}$$

This happens when I and J are large and also when the bare coupling is large. However, in the weak coupling limit with I and J held fixed, χ should have a perturbation expansion

$$\chi(I,J) = C_1 g_o^2 + O(g_o^4) \tag{5.5}$$

For example,

$$\chi(1,1) \underset{g_o^2 \to 0}{\sim} \begin{cases} \frac{3}{16}\, g_o^2 & SU(2) \\ \frac{1}{3}\, g_o^2 & SU(3) \end{cases} \tag{5.6}$$

This power behavior is radically different from the essential singularity expected for the right hand side of eq. (5.4)

$$a^2K \underset{g_o^2 \to 0}{\sim} \frac{K}{\Lambda_o^2} (\gamma_o g_o^2)^{(-\gamma_1/\gamma_o^2)} \exp(-1/(\gamma_o g_o^2)) \tag{5.7}$$

This defines the asymptotic freedom scale Λ_o and is just a rewriting of eq. (1.2). In summary, for strong coupling we expect all $\chi(I,J)$ to equal the coefficient of the area law but, as g_o^2 is reduced, small I and J should give a χ deviating from the desired value. Thus the envelope of curves of $\chi(I,J)$ plotted versus the coupling should give the true value of a^2K.

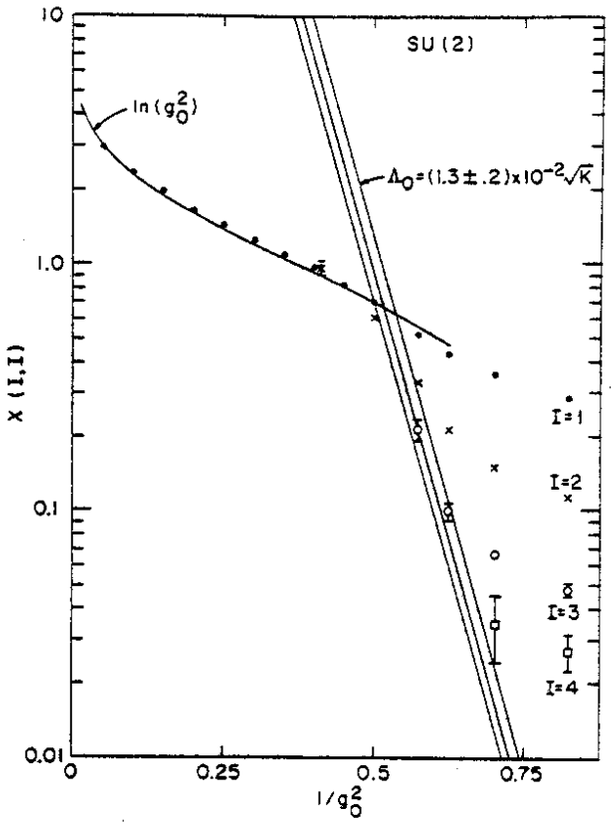

Fig. 4 The quantities $\chi(I,I)$ for SU(2) gauge theory as a function of g_o^{-2}.

In Fig. 4 I plot $\chi(I,I)$ for I = 1-4 versus $1/g_o^2$ for the gauge group SU(2). At strong coupling the large loops have large relative errors but are consistent with χ approaching the values from smaller loops. On this graph I also plot the strong coupling limit for all γ

$$\chi(I,J) = \ell n(g_o^2) + O(g_o^{-4}) \qquad (5.8)$$

The weak coupling behavior of eq. (4.7) is shown as a band corresponding to

$$\Lambda_o = (1.3 \pm .2) \times 10^{-2} \sqrt{K} \qquad (SU(2)) \qquad (5.9)$$

Figure 5 shows the same analysis for SU(3). Here the strong coupling limit is

$$\chi(I,J) = \ell n(3g_o^{\,2}) + O(g_o^{\,-2}) \tag{5.10}$$

and the band for Λ_o is

$$\Lambda_o = (5.0 \pm 1.5) \times 10^{-3}\ \sqrt{K} \quad \text{(SU(3)} \tag{5.11}$$

At first sight the small numbers in eqs. (4.9) and (4.11) were rather surprising, as the pure gauge theories have no small dimensionless parameters. However, the value of Λ_o is strongly dependent on renormalization scheme. Hasenfratz and Hasenfratz[9] have done a perturbative calculation relating this Λ_o to the more conventional Λ^{MOM} defined by the three-point vertex momentum subtracted in Feynman gauge. They find

$$\Lambda^{MOM} = 57.5\ \Lambda_o \quad SU(2) \tag{5.12}$$

$$\Lambda^{MOM} = 83.5\ \Lambda_o \quad SU(3) \tag{5.13}$$

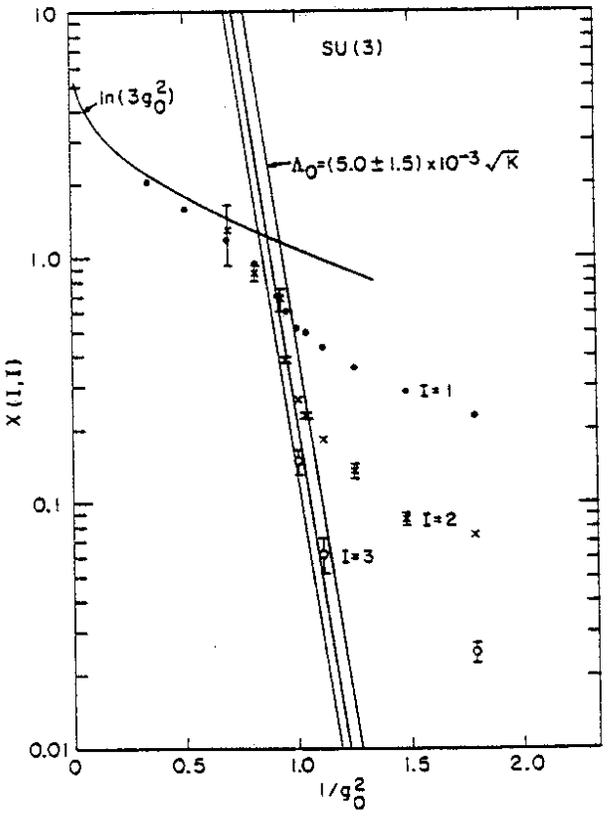

Fig. 5 The quantities $\chi(I,J)$ for the SU(3) theory.

These factors largely compensate for the small numbers for Λ_o. If we accept the string model correction[10] between K and the Regge slope α'

$$K = 1/(2\pi\alpha') \tag{5.14}$$

and use $\alpha' = 1.0\ (\text{GeV})^{-2}$, then we conclude for SU(3)

$$\Lambda^{\text{MOM}} = 170 \pm 50\ \text{MeV} \tag{5.15}$$

Phenomenological interpretation of this value requires an understanding of the neglected effects of virtual quark loops.

THE CONTINUUM LIMIT AND THE RENORMALIZATION GROUP

One of the marvelous features of Monte Carlo simulation is that the entire lattice is stored in the computer memory and therefore one can in principle measure any desired function of the fields. Indeed, the most difficult part of this technique is deciding just what to measure. Of course, we are ultimately interested in taking the continuum limit of our lattice theory. Renormalization group techniques tell us how to adjust the coupling constant for this limit. Non-Abelian gauge theories are asymptotically free, which for our purposes means that the bare charge must be taken to zero.[11] This should be done in such a manner that physical observables remain finite. In this section I will review the renormalization group prediction, and then present some Monte Carlo measurements verifying asymptotic freedom.

In a conventional perturbative treatment, one defines a renormalized coupling g_R in terms of a physical observable at a scale of mass μ. The precise definition is merely a convention, but to lowest order it should agree with the bare charge

$$g_R(g_o,\mu,a) = g_o + O(g_o^3) \tag{6.1}$$

where a is the lattice spacing or cutoff scale. The variation of g_R with the scale of definition gives rise to the Gell-Mann Low function

$$\gamma(g_R) = -\mu \frac{\partial}{\partial \mu} g_R \ (g_o, \mu, a) \tag{6.2}$$

If the continuum limit is physically sensible, then $\gamma(g_R)$ should remain a finite function as a is taken to zero. For SU(N) a perturbative evaluation of $\gamma(g_R)$ gives

$$\gamma(g_R) = \gamma_o {g_R}^3 + \gamma_1 {g_R}^5 + O({g_o}^7) \tag{6.3}$$

where γ_o and γ_1 are independent of renormalization scheme and have the values[12]

$$\gamma_o = \frac{11}{3} (N/16\ \pi^2) \tag{6.4}$$

$$\gamma_1 = \frac{34}{3} (N/16\ \pi^2)^2 \tag{6.5}$$

Remarkably, if a perturbative analysis is ever valid, then eq. (6.3) tells us how g_o must be varied as a function of a for a continuum limit. In this limit, the renormalized g_R should not vary; thus, we conclude

$$0 = a \frac{d}{da} g_R(g_o, \mu, a) = a \frac{\partial g_R}{\partial a} + \frac{\partial g_R}{\partial g_o} a \frac{\partial g_o}{\partial a} \tag{6.6}$$

Simple dimensional analysis tells us

$$a \frac{\partial g_R}{\partial a} = \mu \frac{\partial g_R}{\partial \mu} = \gamma(g_R) \tag{6.7}$$

Combining the previous equations gives

$$a \frac{\partial g_o}{\partial a} = \gamma(g_o) + O({g_o}^7) \tag{6.8}$$

A little algebra shows that the $O({g_o}^5)$ corrections cancel in this equation. Indeed, dropping the corrections in eq. (6.8) gives rise to a definition of an alternative Gell-Mann Low function.

If $g_o(a)$ is ever small enough that $O({g_o}^7)$ terms can be neglected in eq. (6.8), then we can integrate to obtain -

$${g_o}^2(a) = (\gamma_o \ell n(1/({\Lambda_o}^2 a^2)) + (\gamma_1/\gamma_o) \ell n(\ell n(1/({\Lambda_o}^2 a^2))) + O({g_o}^2))^{-1} \tag{6.9}$$

Here Λ_o is an integration constant which determines the scale of a logarithmic decrease of ${g_o}^2$ as the lattice spacing is reduced.

We would like to check this logarithmic decrease with our Monte Carlo simulation. In particular, if we measure some general

physical observable P as a function of g_o, a, and the scale $r = \mu^{-1}$,

$$P = P(r,a,g_o(\mu)) \tag{6.10}$$

then P should not change as we vary a and g_o in the way indicated in eq. 6.9. Thus, for a factor of two change in cutoff we expect

$$P(r,\tfrac{a}{2},g_o(\tfrac{a}{2})) = P(r,a,g_o(a)) + O(a^2) \tag{6.11}$$

In general, there are two classes of dimensional parameters which set the scale for the finite cutoff corrections in this equation. First is the scale r used to define P. As our lattices in practice are rather small, these corrections must be optimistically ignored. Second, there are the dimensional parameters characterizing the continuum theory. Regardless of the value of r, we expect corrections of order a^2m^2 where m is a typical hadronic mass. One should not trust the lattice theory phenomenologically when the lattice spacing is larger than a proton.

Assuming P is dimensionless, we can scale a factor of two from both r and a to obtain

$$P(2r,a,g_o(\tfrac{a}{2})) = P(r,a,g_o(a)) \tag{6.12}$$

Thus a measurement at two different physical scales relates the bare coupling at two values of cutoff.

The most studied "order parameter" in lattice gauge theory is the Wilson loop.[2] We would like to use the loops to define a physical observable. Unfortunately, the bare loop at finite fixed size cannot be used because of ultraviolet divergences. These are of a rather trivial nature, arising from the infinitely thin contour. They represent the self energy of pointlike sources circumnavigating the loop. To proceed, we assume that removing divergences proportional to the loop perimeter and divergences from sharp corners, inevitable in our lattice formulation, as well as appropriately renormalizing the bare charge, will leave the finite physical part of the Wilson loop. This immediately implies that ratios of loops with the same perimeter and number of corners remain finite in the continuum limit. Thus motivated, we define the two functions of bare coupling[13]

$$F(g_o) = 1 - \frac{W(2,2)\ W(1,1)}{(W(1,2))^2} \tag{6.13}$$

and

$$G(g_o) = 1 - \frac{W(4,4)\ W(2,2)}{(W(2,4))^2} \tag{6.14}$$

Here W(I,J) is a rectangular Wilson loop of dimensions I by J in lattice units.

In eq. (6.13) we have effectively taken r = 2a in the more general ratio

$$P(r,a,g_o) = 1 - \frac{W(\frac{r}{a},\frac{r}{a})\ W(\frac{r}{2a},\frac{r}{2a})}{(W(\frac{r}{a},\frac{r}{2a}))^2} \tag{6.15}$$

For small g_o this can be expanded perturbatively

$$P(r,a,g_o) = p_1 g_o^{\,2} + O(g_o^{\,4}) + O(\frac{a^2}{r^2}\, g_o^{\,2}) \tag{6.16}$$

where for SU(2)

$$p_1 = \frac{3}{16\pi^2}\left[8 \arctan 2 + 2 \arctan \frac{1}{2} - 2\pi - 4 \ln(\frac{5}{4})\right] \tag{6.17}$$

$$= 0.049559841....$$

Conversely, in the strong coupling limit

$$F(g_o) = 1 - \frac{1}{g_o^{\,2}} + O(g_o^{\,-6}) \tag{6.18}$$

$$G(g_o) = 1 - \frac{1}{g_o^{\,8}} + O(g_o^{\,-12}) \tag{6.19}$$

In Fig. 6 I show the Monte Carlo results for the functions F and G of eqs. (6.13) and (6.14). Note that the function G always appears to lie above F and that both functions are monotonic increasing in $g_o^{\,2}$. Thus we conclude from eq. (6.12) that the bare charge is a monotonic function of the cutoff, decreasing to zero as the cutoff is removed. In this figure I also show the weak coupling limit of eq. (6.16) and the strong coupling limits in eqs. (6.18) and (6.19).

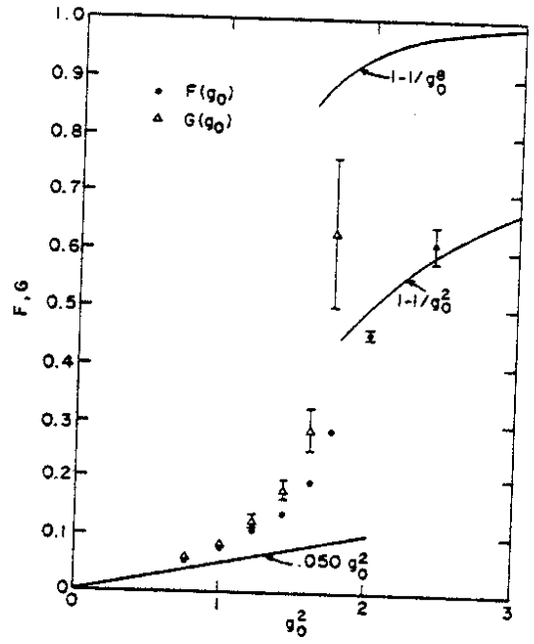

Fig. 6 The ratios F and G as functions of the SU(2) coupling.

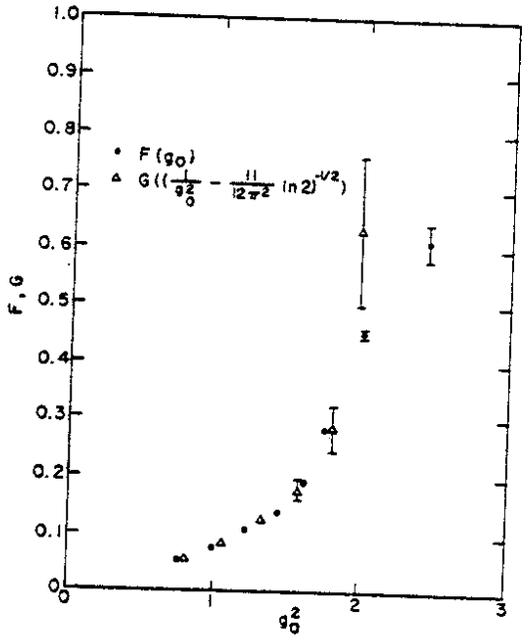

Fig. 7 Testing asymptotic freedom.

Asymptotic freedom predicts a logarithmic decrease of g_o^2 with cutoff when we approach the continuum theory. Using eq. (6.9), we thus expect

$$F(g_o) = G((\frac{1}{g_o^2} - \frac{11}{12\pi^2} \ell n 2)^{-1/2} + O(g_o^3)) \tag{6.20}$$

In Fig. 7 I show the function F and G plotted again versus g_o^2 but with G shifted by the amount indicated in eq. (6.20). Note the excellent agreement with the asymptotic freedom prediction. This is rather astonishing in the light of neglected finite cutoff corrections.

The function P in eq. (6.15) should have a finite continuum limit. Therefore we can use it to define a renormalized charge at scale r. Thus absorbing the higher order terms in eq. (6.16), we define

$$g^2(r) = \lim_{a\to o} P(r,a,g_o(a))/p_1 \tag{6.21}$$

Optimistically assuming a is small enough in our function F, we calculate

$$g^2(r=2a) = F(g_o(a))/p_1 \tag{6.22}$$

In Fig. 8 I plot $g^{-2}(2a)$ versus g_o^{-2}. At large inverse charge these points approach a straight line, for which the unit slope is a test of our neglect of finite cutoff corrections. The intercept of this line measures the Λ parameter associated with this definition of g

$$\frac{1}{g_o^2(a)} - \frac{1}{g^2(2a)} = 2\beta_o \ell n(\frac{2\Lambda}{\Lambda_o}) + O(g_o^2) \tag{6.23}$$

From the graph we obtain

$$\Lambda = 22\ \Lambda_o \tag{6.24}$$

This number is in principle calculable in perturbation theory.

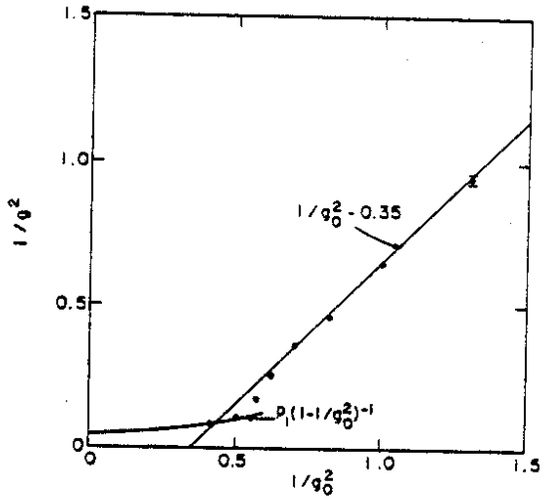

Fig. 8 The inverse renormalized charge squared at r = 2a versus the inverse bare charge squared.

PHASE TRANSITIONS AND VARIANTS ON THE WILSON ACTION

In Fig. 9 I show the results of some Monte Carlo experiments with the gauge group SO(3). Figure 9a is a thermal cycle of this model around $\beta_A = 2.5$. Note the apparent hysteresis effect. Figure 9b shows the results of 100 iteration runs at $\beta_A = 2.5$ from ordered and disordered initial states. Note the appearance of two distinct stable phases. The action per plaquette is normalized

$$S_\square = \beta_A(1 - \tfrac{1}{3}\,\mathrm{Tr}U_\square) \tag{7.1}$$

where $U_\square$ is the product of the SO(3) matrices around the plaquette in question. The quantity P plotted in Fig. 9 is the expectation value of $S_\square$. Thus SO(3) lattice gauge theory has a first order phase transition.[14] This is rather peculiar in that the continuum SO(3) and SU(2) gauge theories are identical.

In Fig. 10 I show the results of four Monte Carlo runs with the gauge group SU(5) at $g_o^{-2} = 1.67$. The upper and lower runs are from random and ordered starts, respectively. The intermediate runs are from superheated and supercooled states. The appearance of two

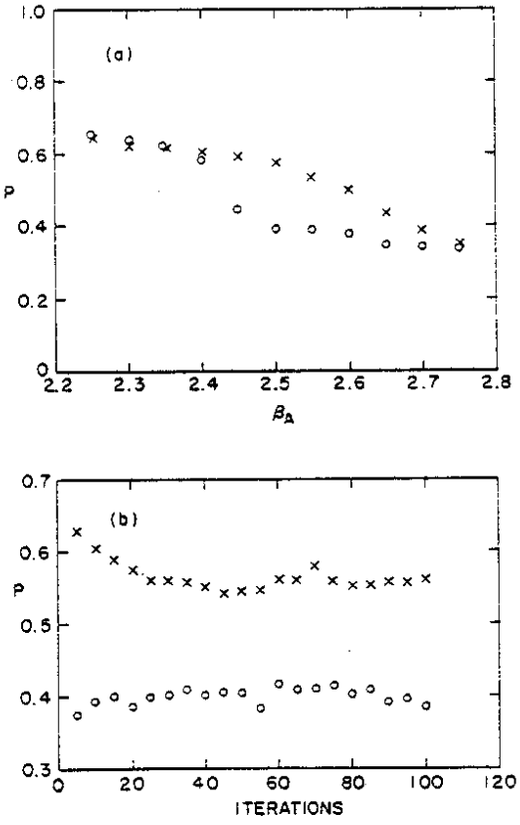

Fig. 9 a. A thermal cycle on the SO(3) model on a 5^4 lattice.
b. Evolution of the SO(3) model at $\beta_A = 2.5$ from ordered and disordered initial states.

distinct asymptotic values for P is indicative of a first order phase transition in this system as well.[15] The critical coupling is $g_o^{-2} = 1.66 \pm 0.03$.

As these groups are non-Abelian, these transitions are presumably not simple deconfinement. One possibility is that they represent a dynamical symmetry breakdown into smaller gauge groups. More mundanely, they might all be artifacts of the lattice action. To see that a change in formulation can modify the phase structure of a gauge theory, Bhanot and I have studied the SU(2) theory with the more general action.[16]

$$S = \beta(1-1/2\ \mathrm{Tr}U_{\square}) + \beta_A(1-1/3\ \mathrm{Tr}_A U_{\square}) \qquad (7.2)$$

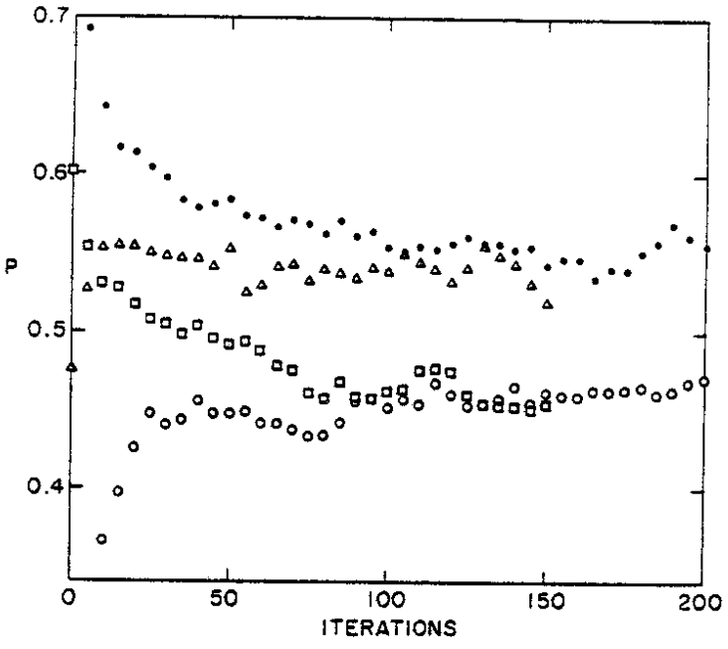

Fig. 10 Four Monte Carlo runs with the gauge group SU(5) at $\beta = 1.67$.

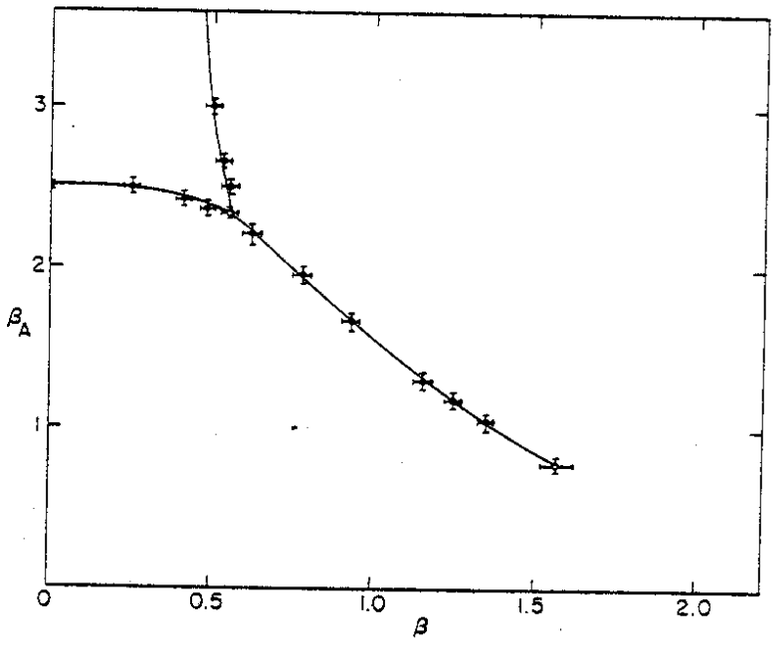

Fig. 11 The phase diagram with the generalized SU(2) action.

Here the first term is the usual Wilson action and in the second the trace Tr_A is taken in the adjoint representation of SU(2). This model has three simple limits: (1) $\beta_A = 0$ is the usual SU(2) theory, (2) $\beta = 0$ is the SO(3) model, and (3) $\beta_A \to \infty$ reduces to Z_2 lattice gauge theory at inverse temperature β. Both limits (2) and (3) have non-trivial phase structure.

Using Monte Carlo techniques, we have obtained the phase diagram shown in Fig. 11. Both the Z_2 and SO(3) transition are stable and meet at a triple point located at

$$(\beta,\beta_A) = (0.55 \pm 0.03,\ 2.34 \pm 0.03) \tag{7.3}$$

A third first order line emerges from this point and ends at a critical point at

$$(\beta,\beta_A) = (1.57 \pm 0.05,\ 0.78 \pm 0.05) \tag{7.4}$$

The conventional SU(2) theory exhibits a narrow but smooth peak in its specific heat[17] at $\beta = 2.2$. This is directly in line with a naive extrapolation of the above first-order transition to the β axis. Thus this peak is a remnant of that transition and a shadow of the nearby critical point.

The continuum SU(2) theory should be unique for all physical observables. The connection between the bare field theoretical coupling and the parameter (β,β_A) is

$$g_o^{-2} = \beta/4 + 2\beta_A/3 \tag{7.5}$$

A continuum limit requires $g_o^2 \to 0$; however, this can be done along many paths in the (β,β_A) plane. Previously we concentrated on the trajectory $\beta_A = 0$, $\beta \to \infty$. Along that line no singularities are encountered and thus confinement, present in strong coupling, should persist into the weak coupling domain. However, an equally justified path would be, for example, $\beta = \beta_A \to \infty$. In this case we cross a first order transition. Because one can continue around it in our larger coupling constant space, the transition is not deconfining and is simply an artifact of the lattice action.

To test whether physical observables are indeed independent of direction in the (β,β_A) plane, we measured Wilson loops in the weak coupling regime for several values of β_A. The loop by itself is not an observable, for reasons discussed previously. As then, we constructed ratios of loops with the same perimeters and numbers of corners. Thus we define

$$R(I,J,K,L) = \frac{W(I,J)\ W(K,L)}{W(I,L)\ W(J,K)} \tag{7.6}$$

Wishing to compare points which give similar physics, we searched at each value of β_A for the values of β for which R(2,2,3,3) had the values 0.87 and 0.93. This gave the points in the (β,β_A) plane shown in Fig. 12. The dashed lines in this figure represent constant bare charge from eq. (7.5). If physics is indeed similar at the corresponding points, then all ratios R of eq. (7.6) should match.

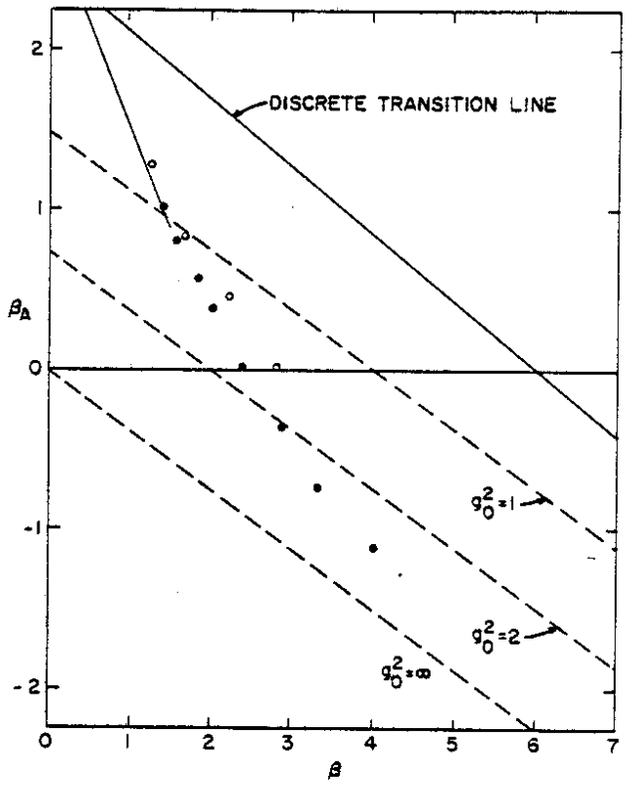

Fig. 12 Points of "constant physics". The solid points give R(2,2,3,3) = 0.87 and the open circles give R(2,2,3,3) = 0.93.

In Fig. 13 I show several such ratios as functions of β_A and at the R(2,2,3,3) = 0.87 points from above. The comparison is quite good considering that finite cutoff corrections are ignored.

Note that in this comparison the bare charge is far from being a constant. In Fig. 12 we see that g_o^2 varied from less than unity to nearly 4 while holding R(2,2,3,3) fixed at 0.87. Such variation is permissible and perhaps even expected since the bare charge is unobservable and should depend on the cutoff prescription. The dependence can be characterized by a β_A dependent renormalization scale defined as in eq. (3.9). Using this relationship, I show in Fig. 14 Λ_o as a function of β_A. Note the consistency of the R(2,2,3,3) = 0.93 and 0.87 results. Remarkably, the addition of

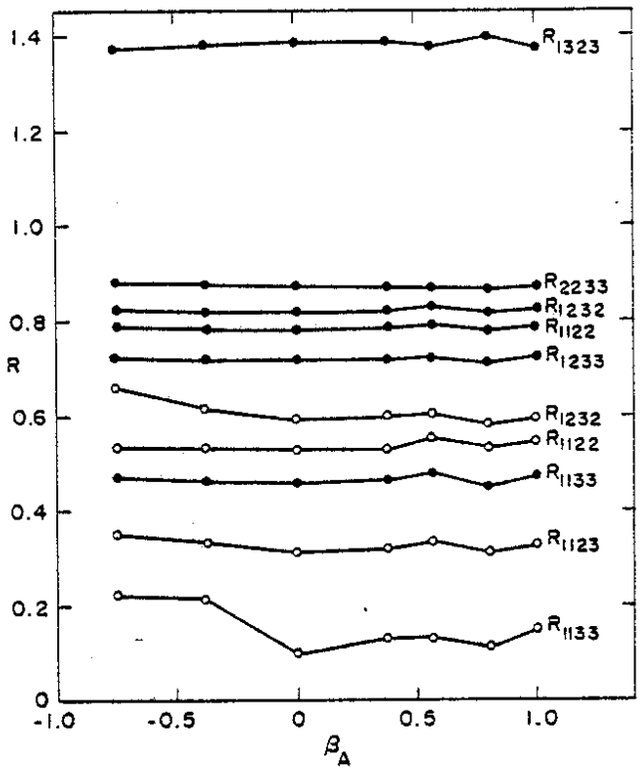

Fig. 13 Physical ratios along the R(2,2,3,3) = 0.87 contour. Solid circles are from loops in the fundamental representation, open circles from the adjoint.

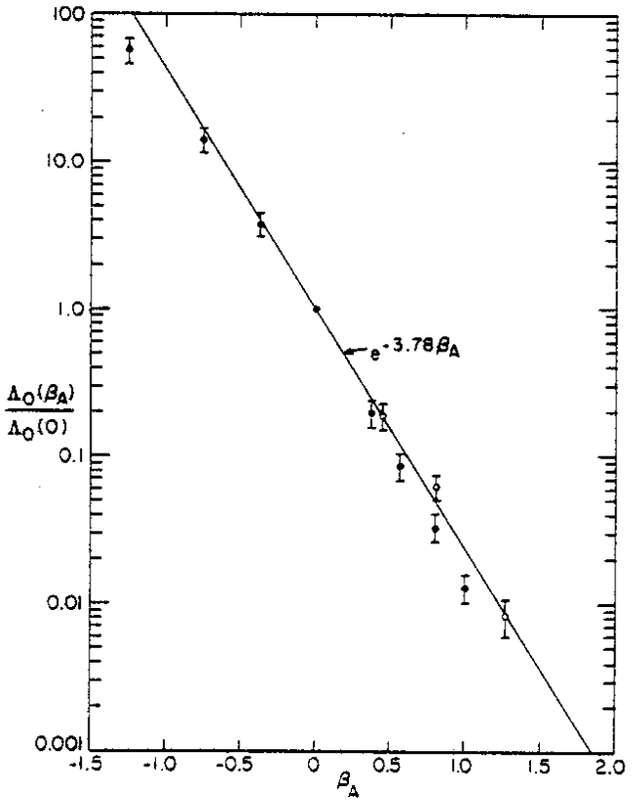

Fig. 14 The β_A dependence of the renormalization scale. The solid circles and open circles are from R(2,2,3,3) = 0.87 and 0.93, respectively.

β_A can change Λ_o by several orders of magnitude. This dependence can in principle be checked with a perturbative calculation.

CONCLUDING REMARKS

I hope to have conveyed to you that lattice gauge theory is both an exciting and a rapidly evolving technique for the particle physicist. We are coming frighteningly close to calculating some real numbers for the strong interactions. The main stumbling block at this stage is the inclusion of light quarks. Courageous attempts at such calculations are being made, however, at present these are severely demanding on computer time and only practical on the most modest lattices. Technical breakthroughs are likely in this area.

REFERENCES

1. M. Gell-Mann and F. E. Low. Phvs. Rev. 95:1300 (1954); W. E. Caswell, Phys. Rev. Lett. 33:244 (1974); D. R. T. Jones, Nucl. Phys. B75:531 (1974).
2. K. Wilson, Phys. Rev. D19:2445 (1974).
3. C. N. Yang and R. Mills, Phys. Rev. 96:191 (1954).
4. M. Creutz, Phys. Rev. D21:2308 (1980).
5. K. Binder, in "Phase Transitions and Critical Phenomena", C. Domb and M. S. Green, eds., Academic Press, New York (1976), Vol. 5B.
6. M. Creutz, Phys. Rev. Lett. 43:553 (1979).
7. B. Lautrup and M. Nauenberg, Phys. Lett. 95B:63 (1980); T. A. Degrand and D. Toussaint, Preprint UCSB-TH-26 (1981); G. Bhanot, Preprint BNL 29087 (1981).
8. M. Creutz, Phys. Rev. Lett. 45:313 (1980).
9. A. Hasenfratz and P. Hasenfratz, Phys. Lett. 93B:165 (1980).
10. P. Goddard, J. Goldstone, C. Rebbi, and C. B. Thorn, Phys. Rev. D20:2096 (1979).
11. H. D. Politzer, Phys. Rev. Lett. 30:1343 (1973); D. Gross and F. Wilczek, Phys. Rev. Lett. 30:1346 (1973) and Phys. Rev. D8: 3633 (1973).
12. W. E. Caswell, Phys. Rev. Lett. 33:244 (1974); D. R. T. Jones, Nucl. Phys. B75:531 (1974).
13. M. Creutz, Phys. Rev. D23:1815 (1980).
14. I. G. Halliday and A. Schwimmer, Preprint ICTP/80/81-15, (1981); J. Greensite and B. Lautrup, Preprint NBI-HE-81-4, (1981).
15. M. Creutz, Phys. Rev. Lett. 46:1441 (1981); for further analysis see H. Bohr and K. Moriarty, ICTP/80/81-19 (1981).
16. G. Bhanot and M. Creutz, preprint (1981).
17. B. Lautrup and M. Nauenberg, Phys. Rev. Lett. 45:1755 (1980).